

Human PSF concentrates DNA and stimulates duplex capture in DMC1-mediated homologous pairing

Yuichi Morozumi¹, Ryohei Ino¹, Motoki Takaku¹, Mihoko Hosokawa²,
Shinichiro Chuma^{2,3} and Hitoshi Kurumizaka^{1,*}

¹Laboratory of Structural Biology, Graduate School of Advanced Science and Engineering, Waseda University, 2-2 Wakamatsu-cho, Shinjuku-ku, Tokyo 162-8480, ²Institute for Integrated Cell-Material Sciences and ³Institute for Frontier Medical Sciences, Kyoto University, 53 Kawahara-cho, Shogoin, Sakyo-ku, Kyoto 606-8507, Japan

Received August 23, 2011; Revised and Accepted November 23, 2011

ABSTRACT

PSF is considered to have multiple functions in RNA processing, transcription and DNA repair by mitotic recombination. In the present study, we found that PSF is produced in spermatogonia, spermatocytes and spermatids, suggesting that PSF may also function in meiotic recombination. We tested the effect of PSF on homologous pairing by the meiosis-specific recombinase DMC1, and found that human PSF robustly stimulated it. PSF synergistically enhanced the formation of a synaptic complex containing DMC1, ssDNA and dsDNA during homologous pairing. The PSF-mediated DMC1 stimulation may be promoted by its DNA aggregation activity, which increases the local concentrations of ssDNA and dsDNA for homologous pairing by DMC1. These results suggested that PSF may function as an activator for the meiosis-specific recombinase DMC1 in higher eukaryotes.

INTRODUCTION

Homologous recombination is an essential process for meiotic cell division I (1,2). Dmc1 is a eukaryotic homolog of the bacterial RecA recombinase, which promotes a key step, homologous pairing, during homologous recombination. *Dmc1*-deficient mice (3–5) and yeast (6) are sterile due to defects in homologous recombination, indicating its essential function in meiotic recombination. In mitosis, homologous recombination is also required for the accurate repair of DNA double-strand breaks (DSBs) (7–10). Since Dmc1 is produced only in meiotic cells, another RecA homolog,

Rad51, is responsible for homologous pairing in mitotic DSB repair through homologous recombination.

Human DMC1, yeast Dmc1 and rice DMC1A and DMC1B actually promote homologous pairing *in vitro* (11–16). In the homologous-pairing step, Dmc1 binds to single-stranded DNA (ssDNA), and the Dmc1–ssDNA complex then binds double-stranded DNA (dsDNA) to form a ternary complex called the synaptic complex. In this synaptic complex containing Dmc1, ssDNA and dsDNA, the homologous sequences between ssDNA and dsDNA are searched, and a heteroduplex is formed between the incoming ssDNA and the complementary strand of dsDNA. Previous biochemical studies revealed that the human, mouse and yeast Hop2–Mnd1 complexes (17–21), the yeast Swi5–Sfr1 complex (22), human RAD54B (14,23,24) and RAD51AP1 (25) stimulate homologous pairing mediated by Dmc1. These proteins also stimulate the Rad51-mediated homologous pairing (17,18,20,22,26–28). Meiotic cells produce both Dmc1 and Rad51; however, the functional difference between them has not been elucidated. Ancillary factors that induce the distinct functions of Dmc1 and Rad51 may exist for the proper regulation of these DNA recombinase activities during meiotic processes.

Polypyrimidine tract binding protein associated splicing factor (PSF, encoded by the *SFPQ* gene) is a multifunctional protein involved in pre-mRNA processing (29–31), transcription regulation (32–36) and DNA repair (37–39). Previously, we reported that PSF directly interacts with RAD51, and modulates the RAD51-mediated homologous pairing (40). PSF also reportedly interacts with RAD51D, a RAD51 paralog, and is required for DNA repair through homologous recombination between sister chromatids (41). In addition, PSF was identified as a protein that promotes homologous pairing between ssDNA and dsDNA in HeLa cell nuclear extracts (42). These findings strongly suggest that PSF may function

*To whom correspondence should be addressed. Tel: +81 3 5369 7315; Fax: +81 3 5367 2820; Email: kurumizaka@waseda.jp

as a protein factor required for homologous recombinational DNA repair in mitotic cells. Interestingly, PSF is produced in mouse Sertoli cells, which nourish germ cells (43). These facts suggested that PSF may function in meiotic recombination mediated by DMC1.

In the present study, we found that PSF is expressed in testicular germ cells. Purified human PSF robustly stimulated DMC1-mediated homologous pairing by enhancing synaptic complex formation, probably through its DNA aggregation activity. We also found that PSF affected the DMC1-mediated and RAD51-mediated recombination reactions differently *in vitro*. Therefore, PSF may function to regulate the DMC1 and RAD51 activities during meiotic processes.

MATERIALS AND METHODS

Preparation of testicular samples and immunofluorescence staining

For cryosections, adult mouse (3 months old) testes (Jcl:ICR) were decapsulated and fixed with 2% paraformaldehyde in phosphate buffered saline (PBS) for 3 h at 4°C. The fixed tissues were incubated in 15% sucrose in PBS, followed by 30% sucrose in PBS, then cryo-embedded in optimal cutting temperature (OCT) compound (Sakura Fine Tech, Tokyo, Japan). The frozen blocks were cut into 10- μ m thick sections using a cryostat (Leica, Wetzlar, Germany). Structurally preserved nuclei samples were prepared as described (44). Since male mice initiate meiosis in a relatively synchronous fashion at 2 weeks after birth, we used testicular samples from 2-week-old mice. Briefly, testicular samples were minced in MEM-alpha (GIBCO, Carlsbad, USA) to release the germ cells, and then a drop of a single cell suspension was placed on a slide glass and immediately mixed with 3.7% formaldehyde and 100 mM sucrose in PBS (pH 7.4), to preserve the cellular structures. After air drying at room temperature, the slides were washed with water three times, air dried and stored at -80°C until further use. The primary antibodies used were an anti-PSF mouse monoclonal antibody (P2860, Sigma-Aldrich, St Louis, MO, USA), and anti-DMC1 (sc-22768, Santa Cruz Biotechnology, Santa Cruz, USA), anti-RAD51 (sc-8349, Santa Cruz Biotechnology), anti-DAZL (ab34139, Abcam, Cambridge, UK), anti-STRA8 (ab49602, Abcam) and anti-SYCP3 (45) rabbit polyclonal antibodies. The secondary antibodies were Alexa 488 conjugated anti-mouse and Alexa 568 conjugated anti-rabbit IgGs (Invitrogen, Carlsbad, CA, USA). Nuclei were counterstained with 1 μ g/ml Hoechst 33258 dye (Sigma-Aldrich) or with an antifade solution with DAPI (S36939, Invitrogen.). Images were obtained with a fluorescent microscope (BX61, Olympus, Tokyo, Japan) mounted with a CCD camera (DP70, Olympus).

The immunoprecipitation assay

The mouse testis cells (adult mouse, 3 months old) were resuspended in lysis buffer, containing 20 mM sodium phosphate (pH 8.0), 60 mM NaCl, 0.1 mM EDTA, 0.05% Triton X-100, a protease inhibitor cocktail

(Nakarai Tesque, Kyoto, Japan) and 10% glycerol. After a 15 min incubation on ice, the cell lysate was sonicated, and then centrifuged at 11000g for 5 min at 4°C. The supernatant was collected as a whole-cell extract. The anti-PSF mouse monoclonal antibody (12 μ g, P2860, Sigma-Aldrich) and the testis cell extract (equivalent to $\sim 5 \times 10^6$ cells) were mixed and incubated at 4°C for 3 h. The sample was then mixed with 50 μ l of Dynabeads protein G (DYNAL, Carlsbad, CA, USA), and was incubated at 4°C for 1 h. After the incubation, the immunoprecipitates were washed three times with 1 ml of the lysis buffer, and then eluted with SDS-PAGE sample buffer. The immunoprecipitates were fractionated by 12% SDS-PAGE, and were immunoblotted with an anti-DMC1 rabbit polyclonal antibody and a horseradish peroxidase conjugated anti-rabbit IgG antibody. Signals were detected by using the Amersham ECL Prime Western Blotting Detection Reagent (GE Healthcare Biosciences, Uppsala, Sweden).

Protein purification

Human PSF (40), DMC1 (13), RAD51 (46,47) and HOP2-MND1 (18) were prepared by the methods described previously. Briefly, human PSF, DMC1, RAD51 and HOP2-MND1 were expressed in *Escherichia coli* cells as His₆-tagged proteins, and the His₆ tag was removed by a thrombin protease treatment during the purification procedure.

The pull-down assay with Ni-NTA beads

Purified His₆-tagged PSF (2.1 μ g) was mixed with DMC1 (4 μ g) or RAD51 (4 μ g) in 60 μ l of binding buffer, containing 12 mM sodium phosphate (pH 7.5), 2 mM HEPES-NaOH (pH 7.5), 66 mM NaCl, 25 mM KCl, 0.16 mM EDTA, 1.4 mM 2-mercaptoethanol, 0.025% Triton X-100 and 6.8% glycerol, and Ni-NTA agarose beads (1.5 μ l, 50% slurry) were then added. After an incubation at room temperature for 1 h, the beads were washed twice with 300 μ l of wash buffer, containing 20 mM sodium phosphate (pH 7.5), 100 mM NaCl, 0.25 mM EDTA, 2 mM 2-mercaptoethanol and 10% glycerol. The proteins bound to the beads were fractionated by 15% SDS-PAGE, and the bands were visualized by Coomassie brilliant blue staining.

DNA substrates

In the D-loop formation assay, superhelical dsDNA (pGsat4 DNA) was prepared by a method avoiding alkaline treatment of the cells harboring the plasmid DNA (48,49). For the ssDNA substrate used in the D-loop formation assay, the following oligonucleotide was purchased from Invitrogen, and purified by polyacrylamide gel electrophoresis: 50-mer, 5'-ATT TCA TGC TAG ACA GAA GAA TTC TCA GTA ACT TCT TTG TGC TGT GTG TA-3'. For the homologous-pairing assay with oligonucleotides, the following HPLC-purified DNA oligonucleotides were purchased from Nihon Gene Research Laboratory: 63-mer, 5'-TCC TTT TGA TAA GAG GTC ATT TTT GCG GAT GGC TTA GAG CTT AAT TGC TGA ATC TGG

TGC TGT-3', 32-mer dsDNA, 5'-CCA TCC GCA AAA ATG ACC TCT TAT CAA AAG GA-3' and 5'-TCC TTT TGA TAA GAG GTC ATT TTT GCG GAT GG-3'. For the dsDNA capture assay, the following HPLC-purified DNA oligonucleotides were purchased from Nihon Gene Research Laboratory: 49-mer dsDNA, 5'-GTC CCA GGC CAT TAC AGA TCA ATC CTG AGC ATG TTT ACC AAG CGC ATT G-3' and 5'-CAA TGC GCT TGG TAA ACA TGC TCA GGA TTG ATC TGT AAT GGC CTG GGA C-3'. For the ssDNA protection assay, the following HPLC-purified ssDNA oligonucleotide was purchased from Nihon Gene Research Laboratory: 100-mer, 5'-CTT CGC GAC TCC AGT GAT CGG ACG AGA ACC GGT GCA TTC ACC CTG GTA TAG TCG ACG TCT CTT GCT TGA TGA AAG TTA AGC TAT TTA AAG GGT CAG GGA T-3'. For the synaptic complex formation assay, the following HPLC-purified ssDNA oligonucleotides were purchased from Nihon Gene Research Laboratory: 70-mer homologous ssDNA, 5'-CAT CAG AAA TAT CCG AAA GTG TTA ACT TCT GCG TCA TGG AAG CGA TAA AAC TCT GCA GGT TGG ATA CGC C-3', 70-mer heterologous ssDNA, 5'-GGT GCA TTC ACC CTG GTA TAG TCG ACG TCT CTT GCT TGA TGA AAG TTA AGC TAT TTA AAG GGT CAG GGA T-3'. Single-stranded ϕ X174 viral (+) strand DNA and double-stranded ϕ X174 replicative form I DNA were purchased from New England Biolabs. The linear dsDNA was prepared from the ϕ X174 replicative form I DNA by PstI digestion. All of the DNA concentrations are expressed in moles of nucleotides.

The D-loop formation assay

PSF and/or DMC1 were incubated with the 32 P-labeled 50-mer oligonucleotide (1 μ M) at 37°C for 5 min, in 9 μ l of reaction buffer, containing 20 mM HEPES–NaOH (pH 7.5), 2.0 mM HEPES–KOH (pH 7.5), 4 mM Tris–HCl (pH 8.0), 40 mM NaCl, 50 mM KCl, 0.045 mM EDTA, 0.2 mM 2-mercaptoethanol, 3% glycerol, 5 mM MgCl₂, 1.2 mM DTT, 1 mM ATP, 0.1 mg/ml BSA, 20 mM creatine phosphate and 75 μ g/ml creatine kinase. The reactions were then initiated by the addition of 1 μ l of pGsat4 superhelical dsDNA (30 μ M), and were continued at 37°C for 10 min. The reactions were stopped by the addition of 0.2% SDS and 1.5 mg/ml proteinase K (Roche Applied Science, Basel, Switzerland), and were further incubated at 37°C for 15 min. After adding 6-fold loading dye, the deproteinized reaction products were separated by 1% agarose gel electrophoresis in 1 \times TAE buffer at 4 V/cm for 2 h. The gels were dried and exposed to an imaging plate. The gel images were visualized using an FLA-7000 imaging analyzer (Fujifilm, Tokyo, Japan).

The homologous-pairing assay with oligonucleotides

In this assay, a 63-mer ssDNA and a 32-mer dsDNA, which were commonly employed in previous studies (40,50–53), were used. DMC1 (4 μ M) and the indicated amount of PSF were incubated with a 63-mer ssDNA (15 μ M) at 37°C for 5 min, in 9 μ l of reaction buffer,

containing 22 mM HEPES–NaOH (pH 7.5), 4 mM Tris–HCl (pH 8.0), 40 mM NaCl, 50 mM KCl, 0.045 mM EDTA, 0.2 mM 2-mercaptoethanol, 3% glycerol, 5 mM MgCl₂, 1.2 mM DTT, 1 mM ATP, 0.1 mg/ml BSA, 20 mM creatine phosphate and 75 μ g/ml creatine kinase. The reactions were initiated by the addition of 1 μ l of the 32-mer dsDNA (1.5 μ M), which shared sequence homology with the 63-mer ssDNA. After a 30-min incubation at 37°C, the reaction was stopped by the addition of 0.2% SDS and 1.5 mg/ml proteinase K, and was further incubated at 37°C for 15 min. After 6-fold loading dye was added, the reaction mixtures were subjected to 15% polyacrylamide gel electrophoresis in 0.5 \times TBE buffer (45 mM Tris-base, 45 mM boric acid and 1 mM EDTA). The gels were dried and exposed to an imaging plate. The gel images were visualized using an FLA-7000 imaging analyzer.

The ATPase assay

The ATPase activities of the proteins were analyzed by the release of 32 Pi from [γ - 32 P]ATP. The proteins were mixed with a 49-mer single-stranded oligonucleotide (20 μ M), in 10 μ l of reaction buffer, containing 22 mM HEPES–NaOH (pH 7.5), 2 mM HEPES–KOH (pH 7.5), 6 mM Tris–HCl (pH 8.0), 75 mM NaCl, 50 mM KCl, 0.065 mM EDTA, 5% glycerol, 0.4 mM 2-mercaptoethanol, 1.3 mM DTT, 50 μ M ATP, 5 nCi [γ - 32 P]ATP, 5 mM MgCl₂ and 100 μ g/ml BSA. The protein concentrations were 4 μ M for DMC1 and 1.2 μ M for PSF. The reaction mixtures were incubated at 37°C. At the indicated times, the reaction was stopped by the addition of 0.5 M EDTA, and the products were separated by thin layer chromatography on polyethyleneimine-cellulose in a 0.5 M LiCl and 1 M formic acid solution.

The dsDNA capture assay

DMC1 (4 μ M) and PSF (0.6 μ M) were incubated with a 5'-biotinylated poly dT ssDNA (83-mer, 6 μ M) conjugated to magnetic streptavidin beads at 37°C for 5 min, in 9 μ l of reaction buffer, containing 22 mM HEPES–NaOH (pH 7.5), 4 mM Tris–HCl (pH 8.0), 40 mM NaCl, 20 mM KCl, 0.045 mM EDTA, 0.2 mM 2-mercaptoethanol, 3% glycerol, 5 mM MgCl₂, 1.2 mM DTT, 1 mM ATP, 0.1 mg/ml BSA and 0.01% Nonidet P-40. The reactions were initiated by the addition of 1 μ l of 32 P-labeled heterologous dsDNA (49-mer, 6 μ M), and were continued at 37°C for 10 min. The supernatants were transferred to fresh tubes, and were treated with 0.4% SDS and 1.8 mg/ml proteinase K at 37°C for 15 min. The resulting ssDNA beads were washed twice with 10 μ l of the reaction buffer. The dsDNA captured by the ssDNA beads was extracted by a treatment with 0.4% SDS and 1.8 mg/ml proteinase K at 37°C for 15 min, followed by a phenol/chloroform extraction and was analyzed by 10% polyacrylamide gel electrophoresis in 0.5 \times TBE buffer. The gels were dried and exposed to an imaging plate. The gel images were visualized using an FLA-7000 imaging analyzer.

The ssDNA protection assay

The proteins were incubated with the ^{32}P -labeled 100-mer oligonucleotide (1 μM) at 37°C for 5 min, in 9 μl of reaction buffer, containing 22 mM HEPES–NaOH (pH 7.5), 2 mM HEPES–KOH (pH 7.5), 4 mM Tris–HCl (pH 8.0), 55 mM NaCl, 50 mM KCl, 0.055 mM EDTA, 4% glycerol, 0.4 mM 2-mercaptoethanol, 1.2 mM DTT, 1 mM ATP, 5 mM MgCl_2 and 100 $\mu\text{g/ml}$ BSA. The reactions were initiated by the addition of 5U of exonuclease I (New England Biolabs, Ipswich, MA, USA), and were continued at 37°C for 10 min. The reaction was stopped by the addition of 0.2% SDS and 1.5 mg/ml proteinase K, and was further incubated at 37°C for 15 min. After 6-fold loading dye was added, the reaction mixtures were subjected to 12% polyacrylamide gel electrophoresis in 0.5 \times TBE buffer (45 mM Tris-base, 45 mM boric acid and 1 mM EDTA). The gels were dried and exposed to an imaging plate. The gel images were visualized using an FLA-7000 imaging analyzer.

The synaptic complex formation assay

DMC1 (4 μM) and PSF (0.6 μM) were incubated with a 70-mer oligonucleotide (6 μM) in 9 μl of reaction buffer, containing 20 mM HEPES–NaOH (pH 7.5), 2 mM HEPES–KOH (pH 7.5), 4 mM Tris–HCl (pH 8.0), 40 mM NaCl, 50 mM KCl, 0.045 mM EDTA, 3% glycerol, 0.2 mM 2-mercaptoethanol, 1.2 mM DTT, 1 mM ATP, 5 mM MgCl_2 and 100 $\mu\text{g/ml}$ BSA. After a 5-min incubation at 37°C, 1 μl of the supercoiled ϕX174 dsDNA (30 μM) was added, and the reaction was continued at 37°C for 5 min. DNA cleavage was initiated by the addition of the PstI restriction enzyme (1.13 U). After the PstI treatment, the reaction was stopped by the addition of 0.2% SDS and 1.5 mg/ml proteinase K, and was further incubated at 37°C for 15 min. After adding 6-fold loading dye, the DNA was separated by 1% agarose gel electrophoresis in 1 \times TAE buffer at 3.3 V/cm for 2 h. The bands were visualized by ethidium bromide staining.

The centrifugation assay for the DNA aggregating activity

Proteins were incubated with ϕX174 ssDNA (10 μM) at 37°C for 5 min, in 19 μl of reaction buffer, containing 22 mM HEPES–NaOH (pH 7.5), 2 mM HEPES–KOH (pH 7.5), 4 mM Tris–HCl (pH 8.0), 40 mM NaCl, 50 mM KCl, 0.045 mM EDTA, 0.2 mM 2-mercaptoethanol, 3% glycerol, 5 mM MgCl_2 , 1.2 mM DTT, 1 mM ATP and 0.1 mg/ml BSA. The reactions were then initiated by the addition of 1 μl of linearized ϕX174 dsDNA (10 μM), and were further incubated at 37°C for 10 min. After this incubation, the samples were centrifuged for 3 min at 20 400g at room temperature, and the upper fractions (15 μl) were separated from the bottom fractions (5 μl) of the samples. The DNA was recovered by a treatment with 0.2% SDS and 1.5 mg/ml proteinase K at 37°C for 15 min. After adding 6-fold loading dye, the DNA was separated by 0.8% agarose gel electrophoresis in 1 \times TAE buffer at 4 V/cm for 2.5 h. The bands were visualized by ethidium bromide staining.

RESULTS

PSF is produced in spermatogonia, spermatocytes and spermatids

We immunologically stained mouse adult testis cryosections with an anti-PSF monoclonal antibody. As shown in Figure 1, the PSF antibody stained various cells, such as spermatogonia, spermatocytes and spermatids. Sertoli cells were also stained with the PSF antibody (Figure 1) (43). We tested PSF production during meiotic stages by analyzing DAZL, STRA8 and SYCP3, which are produced in spermatogonia/spermatocytes, spermatogonia/preleptotene spermatocytes and spermatocytes, respectively, as differentiation markers (Supplementary Figure S1). We then confirmed that PSF was constitutively produced in cells at the stages from preleptotene spermatocytes to secondary spermatocytes (Supplementary Figure S1). Therefore, PSF may function in meiotic events in spermatogenesis.

PSF interacts with DMC1 and RAD51

Previously, we reported that PSF directly binds to RAD51, which functions as a recombinase in meiotic and mitotic cells (40). We then tested whether PSF actually binds to DMC1 and/or RAD51 in mouse testis cells, by an immunoprecipitation assay with an anti-PSF antibody. Endogenous mouse DMC1 and/or RAD51 bound to PSF were detected with the anti-human DMC1 polyclonal antibody, which cross-reacts with both mouse DMC1 and RAD51. As shown in Figure 2A, a substantial amount of mouse DMC1 and/or RAD51 was detected in the PSF-bound fraction, suggesting that PSF interacts with DMC1 and/or RAD51 in the mouse testis cell extract. To confirm whether PSF binds DMC1 and/or RAD51, we performed the pull-down assay with purified human proteins. To do so, PSF was purified as a His₆-tagged protein, and PSF-DMC1 binding or PSF-RAD51 binding was detected by the pull-down assay with the Ni-NTA beads. As shown in Figure 2B and C, purified human PSF bound to both human DMC1 and RAD51, suggesting that PSF binds to both DMC1 and RAD51 in testis cells. However, in meiotic spermatocytes, PSF did not exhibit clear co-localization with mouse DMC1 and RAD51 at the (pre)leptotene and zygotene stages, when many DMC1 and RAD51 foci were formed (Supplementary Figure S2). Therefore, PSF may bind to DMC1 and RAD51 before the DMC1/RAD51 foci formation, and may catalytically function with DMC1/RAD51 during homologous recombination processes.

PSF stimulates DMC1-mediated homologous pairing

We then tested the effect of PSF on homologous recombination reactions mediated by DMC1. The D-loop formation assay was employed to detect the DMC1-mediated homologous pairing *in vitro*. In this assay, the homologous pairing between a ^{32}P -labeled 50-mer oligonucleotide and superhelical dsDNA was mediated by DMC1 in an ATP-dependent manner, and the D-loop structure was detected as a homologous-pairing product (Figure 3A).

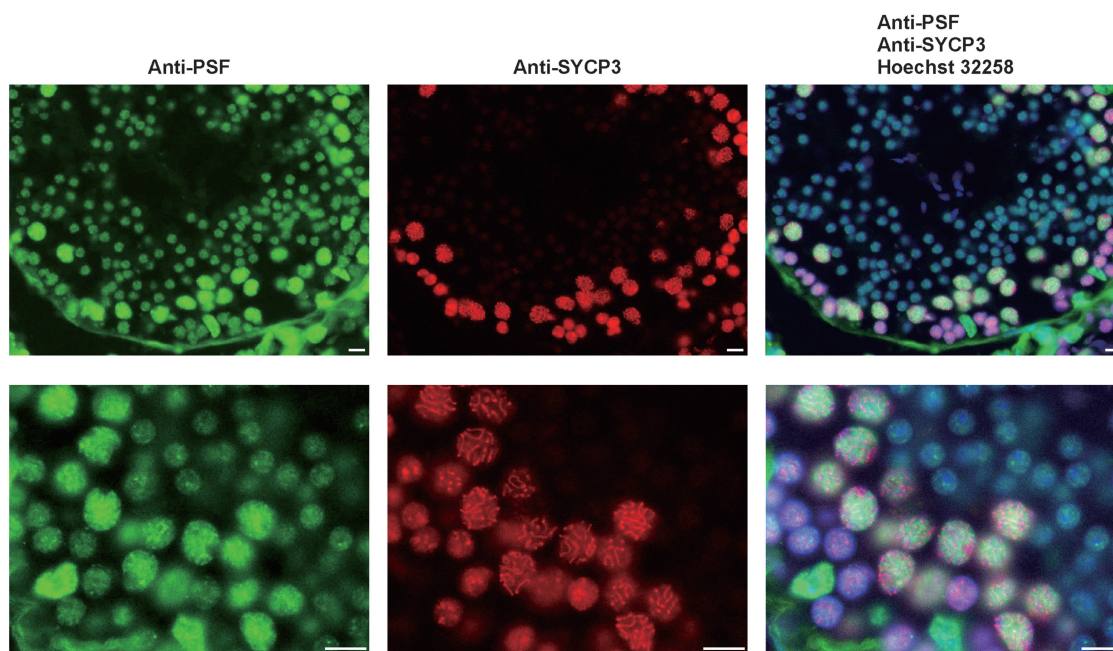


Figure 1. Double immunostaining of mouse testis sections (3 months) for PSF (green) and SYCP3 (red) counterstained with a Hoechst dye (blue). Upper and lower panels are low and high magnification, respectively. Scale bars, 10 μ m.

In the D-loop structure, the 32 P-labeled 50-mer single-stranded oligonucleotide displaces the identical strand of the dsDNA, and forms new Watson–Crick base pairs with its complementary strand.

As shown in Figure 3B (lanes 5–8) and C, we found that purified PSF robustly stimulated the DMC1-mediated D-loop formation in a concentration-dependent manner. PSF alone weakly promoted D-loop formation (Figure 3B, lanes 1–4) (40,42). The omission of ATP did not affect the D-loop formation by PSF alone, but significantly inhibited the DMC1-mediated D-loop formation, regardless of the presence or absence of PSF (Figure 3D). This suggested that PSF actually stimulated the ATP-dependent homologous pairing by DMC1. PSF slightly reduced the ATP hydrolyzing activities of DMC1 in the presence of the 49-mer single-stranded oligonucleotide, but the difference was not significant (Supplementary Figure S3). Since ATP hydrolysis promotes DMC1 dissociation from ssDNA, PSF does not seem to stabilize the DMC1–ssDNA complex by inhibiting ATP hydrolysis and thus reducing its dissociation from ssDNA. Consistently, PSF did not alter the D-loop formation-dissociation kinetics of DMC1, although the yield of D-loops formed by DMC1 was significantly increased in the presence of PSF (Supplementary Figure S4).

We also performed the homologous-pairing assay with a 63-mer single-stranded oligonucleotide and a 32-mer duplex oligonucleotide, in which the displaced strand of the duplex was labeled by 32 P (Figure 3E). Consistent with the results of the D-loop assay, PSF significantly enhanced the DMC1-mediated homologous pairing with this combination of DNA substrates (Figure 3F). Therefore,

we conclude that PSF may function as a *bona fide* activator of DMC1 during meiotic homologous recombination.

PSF stimulates dsDNA capture by the DMC1–ssDNA complex during homologous pairing

We next performed a dsDNA capture assay with the DMC1–ssDNA complex. During homologous pairing, DMC1 forms a ternary complex (synaptic complex), containing ssDNA and dsDNA, and homologous pairing between ssDNA and dsDNA is mediated within this synaptic complex. The synaptic complex formation can be tested by the dsDNA capture assay. DMC1 was incubated with magnetic streptavidin beads conjugated with an 83-mer poly dT ssDNA, and the DMC1–ssDNA complex was formed. The DMC1–ssDNA complexes were then incubated with the 32 P-labeled dsDNA, and the dsDNA incorporated into the synaptic complex was detected by the pull-down assay (Figure 4A) (26). Under the experimental conditions used in this assay, trace amounts of the dsDNA captured by the DMC1–ssDNA complex or the PSF–ssDNA complex were detected (Figure 4B, lanes 2 and 3). In contrast, significant amounts of dsDNA were incorporated into the synaptic complex, when PSF coexisted with DMC1 in the presence of ssDNA (Figure 4B, lane 4). Interestingly, PSF did not enhance the stability of the DMC1–ssDNA and RAD51–ssDNA complexes, as revealed by the ssDNA protection assay with exonuclease I (Figure 4C and D). Therefore, PSF may mainly function in the dsDNA capture step during the DMC1-mediated homologous pairing.

We next performed the restriction enzyme protection assay. In this assay, a dsDNA is protected from cleavage

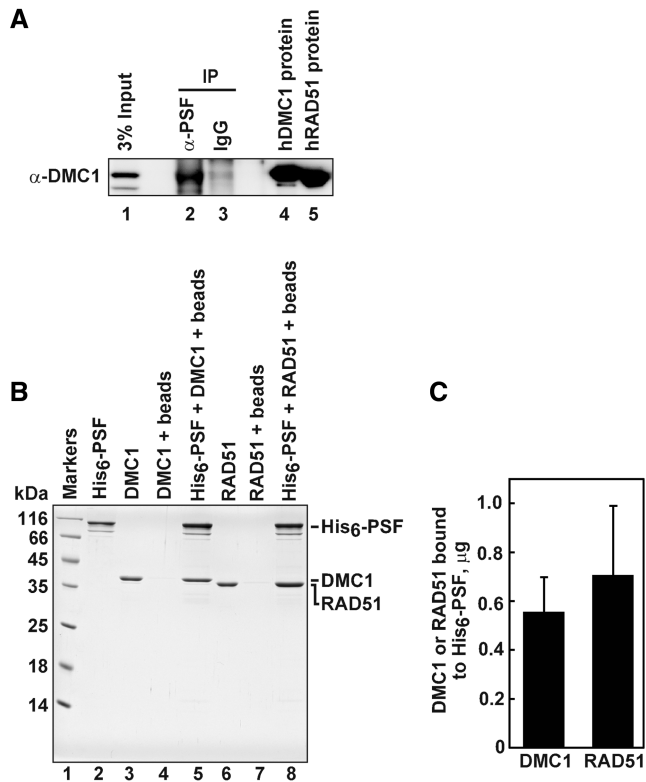


Figure 2. PSF binds to DMC1. (A) The PSF-DMC1/RAD51 interaction was detected in an extract prepared from mouse testis by the pull-down assay with the anti-PSF antibody-conjugated beads. Immunoprecipitates with the anti-PSF antibody were analyzed using an anti-human DMC1 antibody. Lane 1 represents the input (3%). Lane 2 indicates the experiment with the anti-PSF antibody. Lane 3 indicates a negative control experiment with mouse normal IgG. Lanes 4 and 5 show purified protein controls of human DMC1 and RAD51, respectively. (B) The pull-down assay with Ni-NTA beads. Lane 1 represents molecular mass markers. Lanes 2, 3 and 6 show purified protein controls of PSF, DMC1 and RAD51, respectively. Lanes 4 and 7 indicate negative control experiments with DMC1 and RAD51, respectively, in the absence of His₆-tagged PSF. Lanes 5 and 8 indicate experiments with DMC1 and RAD51, respectively, in the presence of His₆-tagged PSF. The proteins bound to His₆-tagged PSF were pulled down by the Ni-NTA agarose beads. The samples were fractionated by 15% SDS-PAGE, and the protein bands were visualized by Coomassie Brilliant Blue staining. (C) Graphic representation of the Ni-NTA agarose bead pull-down assay shown in panel B. The DMC1 and RAD51 band intensities were quantitated, and the average values of three independent experiments are shown with the SD values.

by a restriction enzyme (PstI), if the synaptic complex is formed with the ssDNA containing the homologous sequence of the PstI site by DMC1 and PSF (Figure 4E) (21,54). We found that PSF significantly enhanced the DMC1-mediated synaptic complex formation at the homologous region of the dsDNA (Figure 4F, lanes 2–5, and G). In contrast, the PstI digestion was not prevented when an ssDNA containing a heterologous sequence was used as the substrate for the DMC1-mediated synaptic complex formation (Figure 4F, lanes 6–9, and G). These results suggested that, although the synaptic complex formation occurs in a homology-independent manner, the synaptic complex may be predominantly formed or stabilized on the homologous dsDNA region.

PSF forms DNA aggregates

The bacterial recombinase, RecA, aggregates ssDNA and dsDNA, thus providing DNA fields in which the local concentrations of ssDNA and dsDNA are increased to levels suitable for homologous pairing (55,56). In the present study, we found that PSF possessed DNA aggregation activity. ssDNA and dsDNA were incubated with DMC1 and/or PSF, and the samples were briefly centrifuged at room temperature. The DNA aggregates formed by the proteins were detected in the bottom fraction of the samples (Figure 5A). As shown in Figure 5B, in the presence of ssDNA and dsDNA, DMC1 formed aggregates only with ssDNA (lanes 2 and 6). On the other hand, PSF formed aggregates with both ssDNA and dsDNA, and no DNA was observed in the supernatant (upper) fraction (Figure 5B, lanes 3 and 7). The same result was obtained when PSF and DMC1 coexisted (Figure 5B, lanes 4 and 8). Therefore, we concluded that PSF stimulated dsDNA capture by the DMC1-ssDNA complex, by increasing the local ssDNA and dsDNA concentrations by its aggregation activity.

We compared the DNA aggregation activity of PSF with the HOP2-MND1 complex, which is known to be a *bona fide* auxiliary factor for DMC1 (17–21). Unlike PSF, HOP2-MND1 alone did not form aggregates with ssDNA and dsDNA (Figure 5C, lanes 3 and 7). However, both ssDNA and dsDNA were readily incorporated into aggregates in the presence of DMC1 (Figure 5C, lanes 4 and 8). Although the intrinsic DNA aggregation activity was different between PSF and HOP2-MND1, both auxiliary factors have some similar functions in the presence of DMC1.

DISCUSSION

In the present study, we found that human PSF robustly stimulated DMC1-mediated homologous pairing. PSF enhanced the dsDNA capture by the DMC1-ssDNA complex, probably through ssDNA and dsDNA aggregation (Figure 6). DMC1 alone also exhibited the DNA aggregation activity, but only for ssDNA. Therefore, PSF may be required for efficient dsDNA capture by DMC1, through its aggregation activity for ssDNA and dsDNA. PSF reportedly has weak homologous pairing activity (40,42). This may occur by the spontaneous pairing between ssDNA and dsDNA within the aggregated DNA state produced by PSF.

So far, the Hop2-Mnd1 complexes (17–21), the yeast Swi5-Sfr1 complex (22), human RAD54B (14,23,24) and RAD51AP1 (25) have been reported to stimulate homologous pairing mediated by Dmc1. The Hop2-Mnd1 complex is known to enhance Dmc1-mediated homologous pairing (17–20) in two ways, by stabilizing the Dmc1-ssDNA complex and facilitating the dsDNA capture by the Dmc1-ssDNA complex (21). The HOP2-MND1 complex also reportedly exhibits dsDNA condensing activity (57). Interestingly, we found that the DNA aggregation activity of HOP2-MND1 alone is not apparently significant, but HOP2-MND1 promotes

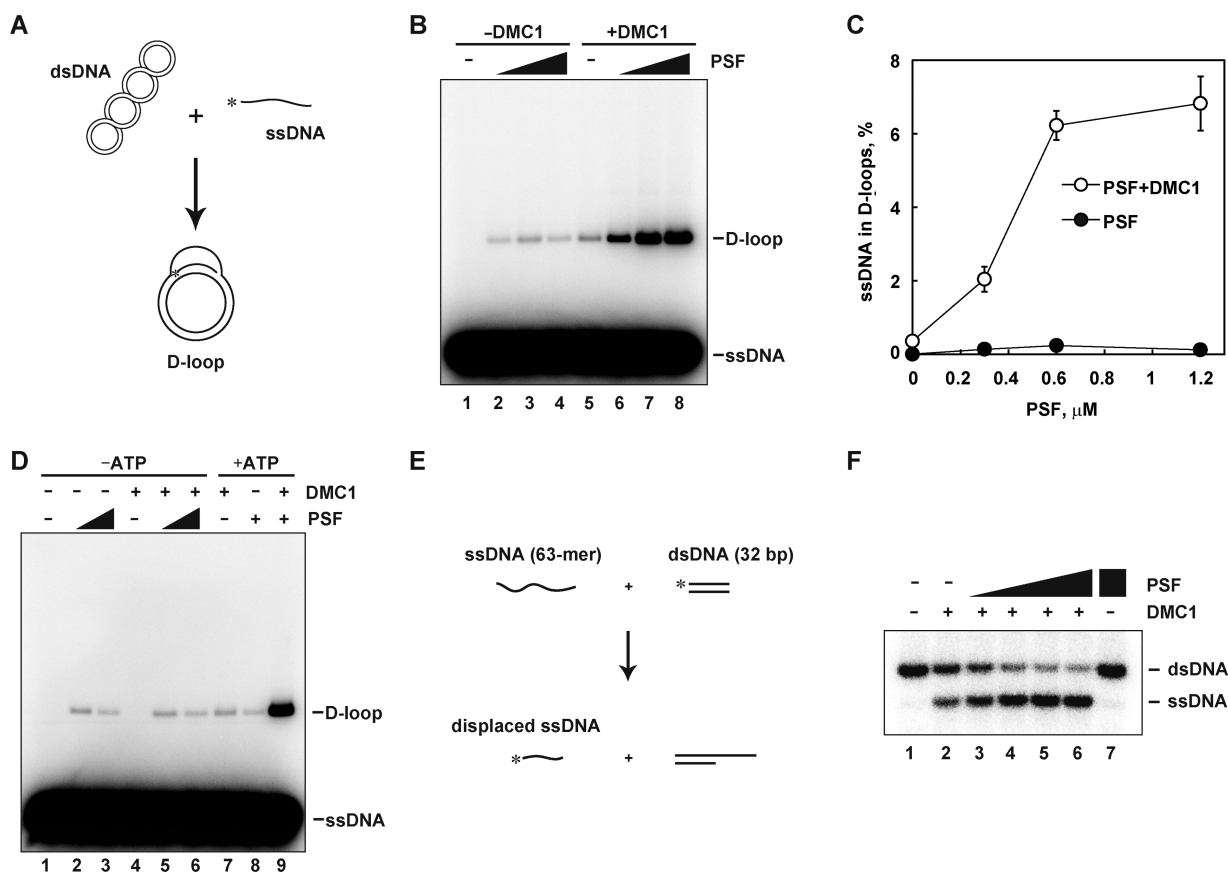


Figure 3. Human PSF stimulates DMC1-mediated homologous pairing. (A) A schematic representation of the D-loop formation assay. Asterisks indicate the ^{32}P -labeled end of the 50-mer ssDNA. (B) The D-loop formation assay. The reactions were conducted without DMC1 (lanes 1–4) or with $4\ \mu\text{M}$ DMC1 (lanes 5–8) in the presence of increasing amounts of PSF. The PSF concentrations were $0\ \mu\text{M}$ (lanes 1 and 5), $0.3\ \mu\text{M}$ (lanes 2 and 6), $0.6\ \mu\text{M}$ (lanes 3 and 7) and $1.2\ \mu\text{M}$ (lanes 4 and 8). (C) Graphic representation of the experiments shown in panel B. The average values of three independent experiments are shown with the SD values. Closed and open circles represent the experiments without and with DMC1, respectively. (D) The D-loop formation assay without ATP. The reactions were conducted without DMC1 (lanes 1–3 and 8) or with $4\ \mu\text{M}$ DMC1 (lanes 4–7 and 9) in the presence of increasing amounts of PSF. The PSF concentrations were $0\ \mu\text{M}$ (lanes 1, 4 and 7), $0.6\ \mu\text{M}$ (lanes 2 and 5) and $1.2\ \mu\text{M}$ (lanes 3, 6, 8 and 9). Lanes 1–6 represent experiments without ATP, and lanes 7–9 represent control experiments with ATP. (E) A schematic representation of the homologous-pairing assay with oligonucleotides. Asterisks indicate the ^{32}P -labeled end of the 32-mer strand, which is complementary to the ssDNA 63-mer. The dsDNA 32-mers were prepared by annealing the ^{32}P -labeled 32-mer strand with the complementary 32-mer. (F) The ssDNA 63-mer ($15\ \mu\text{M}$) was incubated with DMC1 ($4\ \mu\text{M}$) in the presence of the indicated amounts of PSF. The reactions were initiated by adding dsDNA ($1.5\ \mu\text{M}$). Lane 1 indicates a negative control experiment without DMC1, in the presence of PSF ($1.2\ \mu\text{M}$). The PSF concentrations were $0\ \mu\text{M}$ (lane 2), $0.3\ \mu\text{M}$ (lane 3), $0.6\ \mu\text{M}$ (lane 4), $0.9\ \mu\text{M}$ (lane 5) and $1.2\ \mu\text{M}$ (lane 6).

DNA aggregation with DMC1. Similarly, PSF robustly enhanced the dsDNA capture by the DMC1–ssDNA complex, through its DNA aggregation activity. However, PSF did not stabilize the DMC1–ssDNA complex, unlike the HOP2–MND1 complex. RAD51AP1 was identified as a RAD51 associating protein, and enhanced the RAD51-mediated homologous pairing (27,28,58). RAD51AP1 also stimulates dsDNA capture by the DMC1–ssDNA complex (25), but no DNA aggregation activity has been reported. Human RAD54B is an ortholog of the yeast meiotic Rad54 paralog, Tid1/Rdh54 (59,60) and its interactions with DMC1 stimulate the DMC1-mediated recombination reaction, probably by stabilizing the DMC1–ssDNA complex (23,24). Similarly, the yeast Swi5–Sfr1 complex directly binds to Dmc1, and stabilizes the active Dmc1–ssDNA complex (22). Therefore, RAD54B and the

Swi5–Sfr1 complex may primarily function in the Dmc1–ssDNA complex formation step, unlike PSF.

Previously, we reported that PSF modulates RAD51-mediated homologous pairing (40). PSF only stimulates the RAD51-mediated D-loop formation by about 3-fold under conditions with lower amounts of RAD51, and is rather inhibitory with higher amounts of RAD51 (40). However, in the present study, we found that PSF enhanced the yield of D-loops by DMC1, in the presence of both lower and higher amounts of DMC1 (data not shown). With higher PSF or DMC1 concentrations, PSF robustly stimulated DMC1-mediated homologous pairing by about 18-fold. This indicates that DMC1 favors the ssDNA and dsDNA aggregated situation for homologous pairing (Figure 6). In contrast, RAD51 may not properly function in the highly aggregated DNA situation produced by PSF. This difference in the PSF

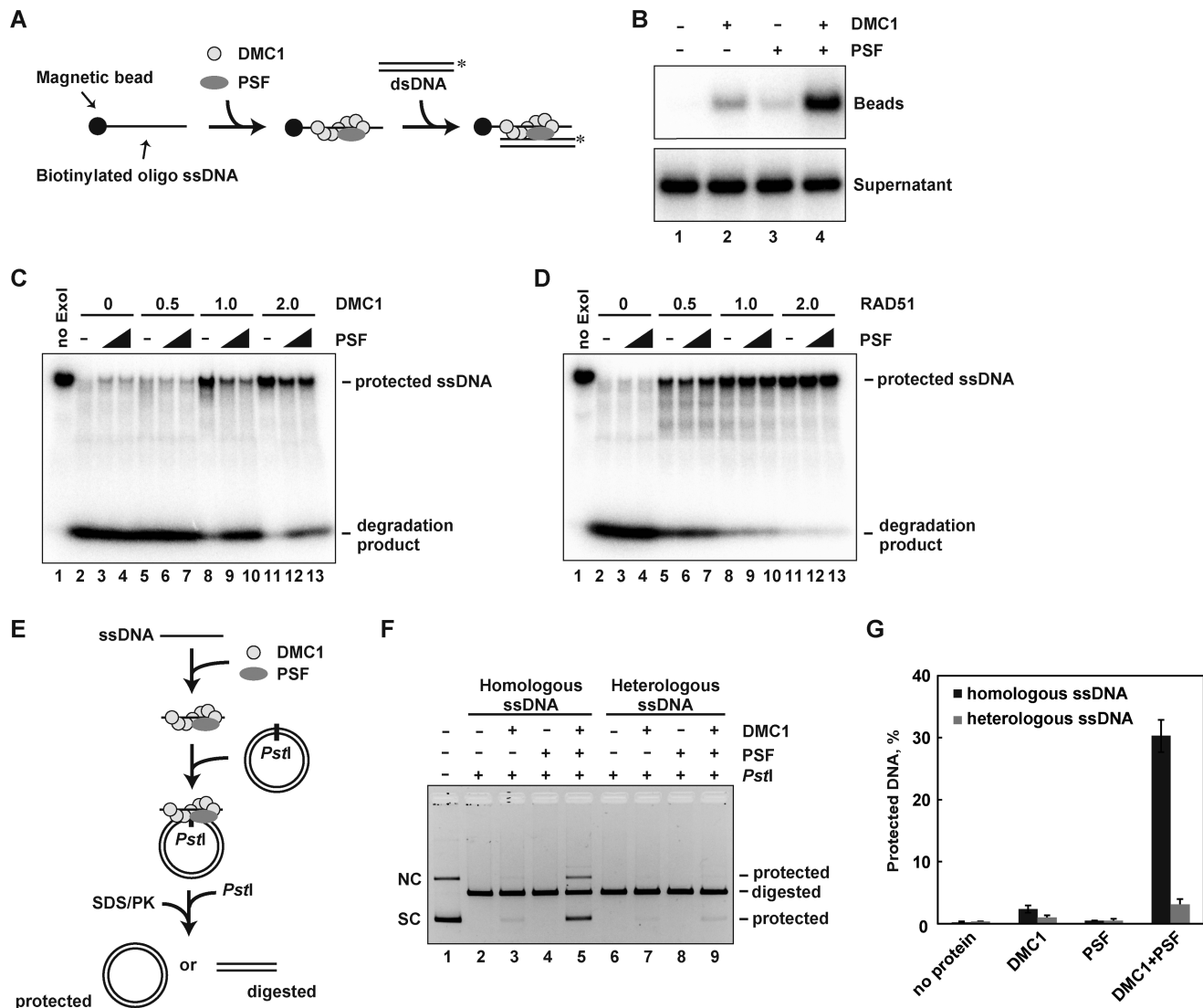


Figure 4. PSF stimulates dsDNA capture by the DMC1-ssDNA complex. (A) Schematic representation of the dsDNA capturing assay. Asterisks indicate the ^{32}P -labeled ends of the dsDNA. (B) The reaction was conducted with DMC1 (4 μM) and/or PSF (0.6 μM), and ^{32}P -labeled dsDNA 49-mer (1.5 μM) in the presence of the 83-mer poly dT ssDNA conjugated to the beads. The dsDNA captured by the DMC1-ssDNA complex was detected. Lane 1 indicates a negative control reaction without the proteins. Lanes 2-4 represent the experiments with DMC1 alone, PSF alone, and both DMC1 and PSF, respectively. Portions including 80% of the dsDNA recovered in the ssDNA bound fraction were analyzed by native PAGE (upper panel), and 10% portions of the dsDNA samples remaining in the ssDNA unbound fraction were analyzed by native PAGE (lower panel). (C) The ssDNA protection assay with DMC1. The DMC1-ssDNA complexes were treated with exonuclease I in the presence or absence of PSF. The resulting ssDNAs were analyzed by native PAGE. Lane 1 indicates a negative control experiment without proteins and exonuclease I. Lanes 3, 6, 9 and 12 indicate experiments with 0.3 μM PSF, and lanes 4, 7, 10 and 13 indicate experiments with 0.6 μM PSF. Lanes 2, 5, 8 and 11 indicate experiments without PSF. The DMC1 concentrations were 0 μM (lanes 2-4), 0.5 μM (lanes 5-7), 1 μM (lanes 8-10) and 2 μM (lanes 11-13). (D) The ssDNA protection assay with RAD51. The reaction was conducted by the same method as in panel C, except RAD51 was used instead of DMC1. (E) Schematic representation of the synaptic complex formation assay. (F) The synaptic complex formation reaction was conducted with DMC1 (4 μM) and/or PSF (0.6 μM), in the presence of the 70-mer ssDNA and superhelical dsDNA. Lane 1 indicates a negative control experiment without proteins and PstI restriction enzyme. Lanes 2 and 6 represent the experiments without proteins. Lanes 2-5 and 6-9 indicate experiments with the homologous ssDNA and heterologous ssDNA, respectively. Lanes 3 and 7 indicate the experiments with DMC1 alone. Lanes 4 and 8 indicate the experiments with PSF alone. Lanes 5 and 9 indicate the experiments with both DMC1 and PSF. NC and SC represent nicked circular and superhelical dsDNA molecules. (G) Graphic representation of the synaptic complex formation assay shown in panel F. The band intensities of the protected DNAs were quantitated, and the average values of three independent experiments are shown with the SD values.

action between DMC1 and RAD51 may be due to the distinctive aspects of their intrinsic DNA binding and/or homologous-pairing activities.

In the present study, we have reported that PSF is a novel DMC1 activating protein. It remains to be clarified how PSF shares the DMC1-stimulating activity with the

previously identified HOP2-MND1 complex, RAD54B and RAD51AP1 in mammals. They may function in distinct chromosomal locations and/or in genomic DNA regions with specific sequence characteristics. These DMC1 activators may function in different steps, such as in DMC1-ssDNA complex formation, synaptic

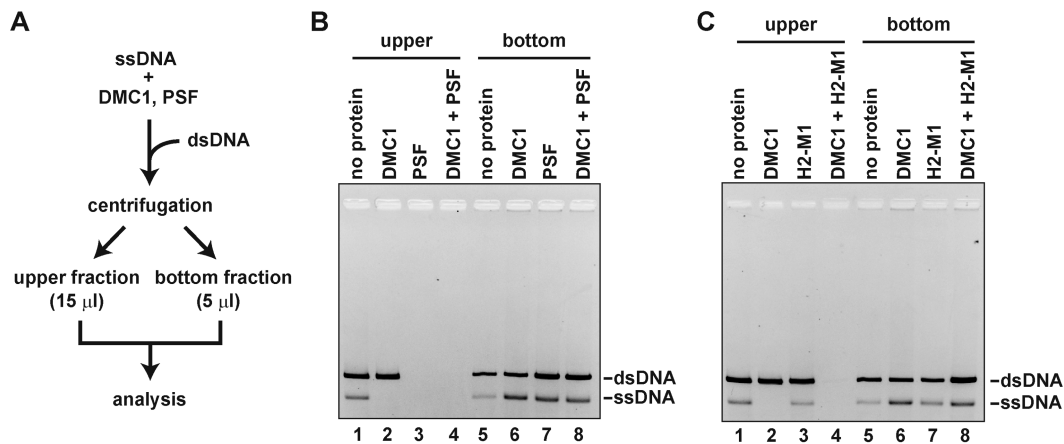


Figure 5. The DNA aggregation assay. (A) Schematic representation of the DNA aggregation assay. (B) The reaction was conducted with DMC1 (4 μ M) and/or PSF (1.2 μ M) in the presence of ϕ X174 ssDNA (10 μ M) and linearized ϕ X174 dsDNA (10 μ M). The samples were centrifuged for 3 min at 20400 g at room temperature, and the ssDNA and dsDNA recovered in the upper (15 μ l) and bottom (5 μ l) fractions were analyzed by 0.8% agarose gel electrophoresis with ethidium bromide staining. (C) The reaction was conducted by the same method as in panel B, except HOP2-MND1 (1.2 μ M) was used instead of PSF.

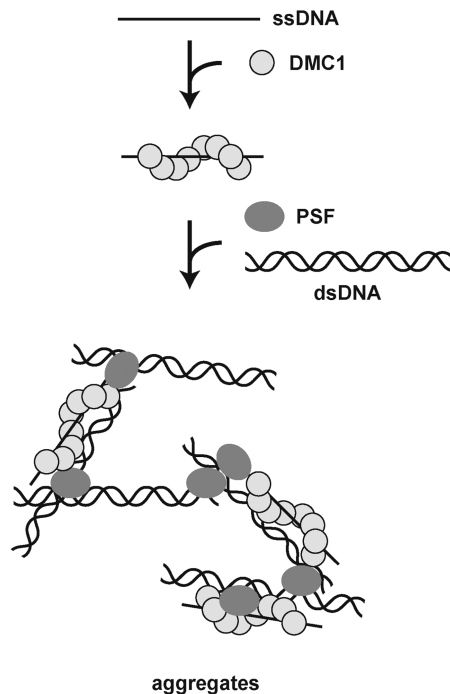


Figure 6. Model of PSF function in DMC1-mediated homologous pairing.

complex formation and heteroduplex formation. Further studies will be required to clarify this issue.

SUPPLEMENTARY DATA

Supplementary Data are available at NAR Online: Supplementary Figures 1–4.

ACKNOWLEDGEMENTS

S.C. and M.H. thank Dr Norio Nakatsuji (Kyoto University) for helpful discussions.

FUNDING

Grants-in-Aid from the Japanese Society for the Promotion of Science (JSPS, partial); Ministry of Education, Culture, Sports, Science and Technology (MEXT), Japan and Waseda Research Institute for Science and Engineering (H.K., research fellow). Funding for open access charge: Waseda University.

Conflict of interest statement. None declared.

REFERENCES

- Petronczki, M., Siomos, M.F. and Nasmyth, K. (2003) Un ménage à quatre: the molecular biology of chromosome segregation in meiosis. *Cell*, **112**, 423–440.
- Neale, M.J. and Keeney, S. (2006) Clarifying the mechanics of DNA strand exchange in meiotic recombination. *Nature*, **442**, 153–158.
- Pittman, D.L., Cobb, J., Schimenti, K.J., Wilson, L.A., Cooper, D.M., Brignull, E., Handel, M.A. and Schimenti, J.C. (1998) Meiotic prophase arrest with failure of chromosome synapsis in mice deficient for *Dmcl*, a germline-specific RecA homolog. *Mol. Cell*, **1**, 697–705.
- Yoshida, K., Kondoh, G., Matsuda, Y., Habu, T., Nishimune, Y. and Morita, T. (1998) The mouse *RecA*-like gene *Dmcl* is required for homologous chromosome synapsis during meiosis. *Mol. Cell*, **1**, 707–718.
- Bannister, A.A., Pezza, R.J., Donaldson, J.R., de Rooij, D.G., Schimenti, K.J., Camerini-Otero, R.D. and Schimenti, J.C. (2007) A dominant, recombination-defective allele of *Dmcl* causing male-specific sterility. *PLoS Biol.*, **5**, 1–10.
- Bishop, D.K., Park, D., Xu, L. and Kleckner, N. (1992) DMC1: a meiosis-specific yeast homolog of *E. coli* recA required for recombination, synaptonemal complex formation, and cell cycle progression. *Cell*, **69**, 439–456.
- Cox, M.M., Goodman, M.F., Kreuzer, K.N., Sherratt, D.J., Sandler, S.J. and Marians, K.J. (2000) The importance of repairing stalled replication forks. *Nature*, **404**, 37–41.
- Symington, L.S. (2002) Role of RAD52 epistasis group genes in homologous recombination and double-strand break repair. *Microbiol. Mol. Biol. Rev.*, **66**, 630–670.
- West, S.C. (2003) Molecular views of recombination proteins and their control. *Nat. Rev. Mol. Cell. Biol.*, **4**, 435–445.

10. San Filippo, J., Sung, P. and Klein, H. (2008) Mechanism of Eukaryotic Homologous Recombination. *Annu. Rev. Biochem.*, **77**, 229–257.
11. Li, Z., Golub, E.I., Gupta, R. and Radding, C.M. (1997) Recombination activities of HsDmc1 protein, the meiotic human homolog of RecA protein. *Proc. Natl Acad. Sci. USA*, **94**, 11221–11226.
12. Hong, E.L., Shinohara, A. and Bishop, D.K. (2001) *Saccharomyces cerevisiae* Dmc1 protein promotes renaturation of single-strand DNA (ssDNA) and assimilation of ssDNA into homologous super-coiled duplex DNA. *J. Biol. Chem.*, **276**, 41906–41912.
13. Kinebuchi, T., Kagawa, W., Enomoto, R., Tanaka, K., Miyagawa, K., Shibata, T., Kurumizaka, H. and Yokoyama, S. (2004) Structural basis for octameric ring formation and DNA interaction of the human homologous-pairing protein Dmc1. *Mol. Cell*, **14**, 363–374.
14. Sehorn, M.G., Sigurdsson, S., Bussen, W., Unger, V.M. and Sung, P. (2004) Human meiotic recombinase Dmc1 promotes ATP-dependent homologous DNA strand exchange. *Nature*, **429**, 433–437.
15. Bugreev, D.V., Golub, E.I., Stasiak, A.Z., Stasiak, A. and Mazin, A.V. (2005) Activation of human meiosis-specific recombinase Dmc1 by Ca²⁺. *J. Biol. Chem.*, **280**, 26886–26895.
16. Sakane, I., Kamataki, C., Takizawa, Y., Nakashima, M., Toki, S., Ichikawa, H., Ikawa, S., Shibata, T. and Kurumizaka, H. (2008) Filament formation and robust strand exchange activities of the rice DMC1A and DMC1B proteins. *Nucleic Acids Res.*, **36**, 4266–4276.
17. Petukhova, G.V., Pezza, R.J., Vanevski, F., Ploquin, M., Masson, J.Y. and Camerini-Otero, R.D. (2005) The Hop2 and Mnd1 proteins act in concert with Rad51 and Dmc1 in meiotic recombination. *Nat. Struct. Mol. Biol.*, **12**, 449–453.
18. Enomoto, R., Kinebuchi, T., Sato, M., Yagi, H., Kurumizaka, H. and Yokoyama, S. (2006) Simulation of DNA strand exchange by the human TBP/Hop2-Mnd1 complex. *J. Biol. Chem.*, **281**, 5575–5581.
19. Pezza, R.J., Petukhova, G.V., Ghirlando, R. and Camerini-Otero, R.D. (2006) Molecular activities of meiosis-specific proteins Hop2, Mnd1, and the Hop2-Mnd1 complex. *J. Biol. Chem.*, **281**, 18426–18434.
20. Ploquin, M., Petukhova, G.V., Morneau, D., Déry, U., Bransi, A., Stasiak, A., Camerini-Otero, R.D. and Masson, J.Y. (2007) Stimulation of fission yeast and mouse Hop2-Mnd1 of the Dmc1 and Rad51 recombinases. *Nucleic Acids Res.*, **35**, 2719–2733.
21. Pezza, R.J., Voloshin, O.N., Vanevski, F. and Camerini-Otero, R.D. (2007) Hop2/Mnd1 acts on two critical steps in Dmc1-promoted homologous pairing. *Genes Dev.*, **21**, 1758–1766.
22. Haruta, N., Kurokawa, Y., Murayama, Y., Akamatsu, Y., Unzai, S., Tsutsui, Y. and Iwasaki, H. (2006) The Swi5-Sfr1 complex stimulates Rhp51/Rad51- and Dmc1-mediated DNA strand exchange *in vitro*. *Nat. Struct. Mol. Biol.*, **13**, 823–30.
23. Sarai, N., Kagawa, W., Kinebuchi, T., Kagawa, A., Tanaka, K., Miyagawa, K., Ikawa, S., Shibata, T., Kurumizaka, H. and Yokoyama, S. (2006) Stimulation of Dmc1-mediated DNA strand exchange by the human Rad54B protein. *Nucleic Acids Res.*, **34**, 4429–4437.
24. Sarai, N., Kagawa, W., Fujikawa, N., Saito, K., Hikiba, J., Tanaka, K., Miyagawa, K., Kurumizaka, H. and Yokoyama, S. (2008) Biochemical analysis of the N-terminal domain of human RAD54B. *Nucleic Acids Res.*, **36**, 5441–5450.
25. Dray, E., Dunlop, M.H., Kauppi, L., San Filippo, J., Wiese, C., Tsai, M.S., Begovic, S., Schild, D., Jasin, M. and Keeney, S. (2011) Molecular basis for enhancement of the meiotic DMC1 recombinase by RAD51 associated protein 1 (RAD51AP1). *Proc. Natl Acad. Sci. USA*, **108**, 3560–3565.
26. Chi, P., San Filippo, J., Sehorn, M.G., Petukhova, G.V. and Sung, P. (2007) Bipartite stimulatory action of the Hop2-Mnd1 complex on the Rad51 recombinase. *Genes Dev.*, **21**, 1747–1757.
27. Modesti, M., Budzowska, M., Baldeyron, C., Demmers, J.A., Ghirlando, R. and Kanaar, R. (2007) RAD51AP1 is a structure-specific DNA binding protein that stimulates joint molecule formation during RAD51-mediated homologous recombination. *Mol. Cell*, **28**, 468–481.
28. Wiese, C., Dray, E., Groesser, T., San Filippo, J., Shi, L., Collins, D.W., Tsai, M.S., Williams, G.J., Rydberg, B. and Sung, P. (2007) Promotion of homologous recombination and genomic stability by RAD51AP1 via RAD51 recombinase enhancement. *Mol. Cell*, **28**, 482–490.
29. Patton, J.G., Porro, E.B., Galceran, J., Tempst, P. and Nadal-Ginard, B. (1993) Cloning and characterization of PSF, a novel pre-mRNA splicing factor. *Genes Dev.*, **7**, 393–406.
30. Kaneko, S., Rozenblatt-Rosen, O., Meyerson, M. and Manley, J.L. (2007) The multifunctional protein p54nrb/PSF recruits the exonuclease XRN2 to facilitate pre-mRNA 3' processing and transcription termination. *Genes Dev.*, **21**, 1779–1789.
31. Buxadé, M., Morrice, N., Krebs, D.L. and Proud, C.G. (2008) The PSF:p54nrb complex is a novel Mnk substrate that binds the mRNA for tumor necrosis factor α . *J. Biol. Chem.*, **283**, 57–65.
32. Urban, R.J., Bodenbun, Y., Kurosky, A., Wood, T.G. and Gasic, S. (2000) Polypyrimidine tract-binding protein-associated splicing factor is a negative regulator of transcriptional activity of the porcine p450scc insulin-like growth factor response element. *Mol. Endocrinol.*, **14**, 774–782.
33. Urban, R.J., Bodenbun, Y.H. and Wood, T.G. (2002) NH₂ terminus of PTB-associated splicing factor binds to the porcine P450scc IGF-I response element. *Am. J. Physiol. Endocrinol. Metab.*, **283**, E423–E427.
34. Urban, R.J. and Bodenbun, Y. (2002) PTB-associated splicing factor regulates growth factor-stimulated gene expression in mammalian cells. *Am. J. Physiol. Endocrinol. Metab.*, **283**, E794–E798.
35. Song, X., Sui, A. and Garen, A. (2004) Binding of mouse VL30 retrotransposon RNA to PSF protein induces genes repressed by PSF: effects on steroidogenesis and oncogenesis. *Proc. Natl Acad. Sci. USA*, **101**, 621–626.
36. Song, X., Sun, Y. and Garen, A. (2005) Roles of PSF protein and VL30 RNA in reversible gene regulation. *Proc. Natl Acad. Sci. USA*, **102**, 12189–12193.
37. Bladen, C.L., Udayakumar, D., Takeda, Y. and Dynan, W.S. (2005) Identification of the polypyrimidine tract binding protein-associated splicing factor p54(nrb) complex as a candidate DNA double-strand break rejoining factor. *J. Biol. Chem.*, **280**, 5205–5210.
38. Salton, M., Lerenthal, Y., Wang, S.Y., Chen, D.J. and Shiloh, Y. (2010) Involvement of matrin 3 and SFPQ/NONO in the DNA damage response. *Cell Cycle*, **9**, 1568–1576.
39. Ha, K., Takeda, Y. and Dynan, W.S. (2011) Sequences in PSF/SFPQ mediate radioresistance and recruitment of PSF/SFPQ-containing complexes to DNA damage sites in human cells. *DNA Repair*, **10**, 252–259.
40. Morozumi, Y., Takizawa, Y., Takaku, M. and Kurumizaka, H. (2009) Human PSF binds to RAD51 and modulates its homologous-pairing and strand-exchange activities. *Nucleic Acids Res.*, **37**, 4296–4307.
41. Rajesh, C., Baker, D.K., Pierce, A.J. and Pittman, D.L. (2011) The splicing-factor related protein SFPQ/PSF interacts with RAD51D and is necessary for homology-directed repair and sister chromatid cohesion. *Nucleic Acids Res.*, **39**, 132–145.
42. Akhmedov, A.T. and Lopez, B.S. (2000) Human 100-kDa homologous DNA-pairing protein is the splicing factor PSF and promotes DNA strand invasion. *Nucleic Acids Res.*, **28**, 3022–3030.
43. Kuwahara, S., Ikei, A., Taguchi, Y., Tabuchi, Y., Fujimoto, N., Obinata, M., Uesugi, S. and Kurihara, Y. (2006) PSCP1, NONO, and SFPQ are expressed in mouse Sertoli cells and may function as coregulators of androgen receptor-mediated transcription. *Biol. Reprod.*, **75**, 352–359.
44. Scherthan, H., Jerratsch, M., Li, B., Smith, S., Hultén, M., Lock, T. and de Lange, T. (2000) Mammalian meiotic telomeres: protein composition and redistribution in relation to nuclear pores. *Mol. Biol. Cell*, **11**, 4189–4203.
45. Chuma, S. and Nakatsuji, N. (2001) Autonomous transition into meiosis of mouse fetal germ cells *in vitro* and its inhibition by gp130-mediated signaling. *Dev. Biol.*, **229**, 468–479.

46. Matsuo, Y., Sakane, I., Takizawa, Y., Takahashi, M. and Kurumizaka, H. (2006) Roles of the human Rad51 L1 and L2 loops in DNA binding. *FEBS J.*, **273**, 3148–3159.
47. Ishida, T., Takizawa, Y., Sakane, I. and Kurumizaka, H. (2008) The Lys313 residue of the human Rad51 protein negatively regulates the strand-exchange activity. *Genes Cells*, **13**, 91–103.
48. Kurumizaka, H., Ikawa, S., Nakada, M., Eda, K., Kagawa, W., Takata, M., Takeda, S., Yokoyama, S. and Shibata, T. (2001) Homologous-pairing activity of the human DNA-repair proteins Xrcc3.Rad51C. *Proc. Natl Acad. Sci. USA*, **98**, 5538–5543.
49. Kagawa, W., Kurumizaka, H., Ikawa, S., Yokoyama, S. and Shibata, T. (2001) Homologous pairing promoted by the human Rad52 protein. *J. Biol. Chem.*, **276**, 35201–35208.
50. Lio, Y.C., Mazin, A.V., Kowalczykowski, S.C. and Chen, D.J. (2003) Complex formation by the human Rad51B and Rad51C DNA repair proteins and their activities in vitro. *J. Biol. Chem.*, **278**, 2469–2478.
51. Takizawa, Y., Kinebuchi, T., Kagawa, W., Yokoyama, S., Shibata, T. and Kurumizaka, H. (2004) Mutational analyses of the human Rad51-Tyr315 residue, a site for phosphorylation in leukaemia cells. *Genes Cells*, **9**, 781–790.
52. Takaku, M., Machida, S., Hosoya, N., Nakayama, S., Takizawa, Y., Sakane, I., Shibata, T., Miyagawa, K. and Kurumizaka, H. (2009) Recombination activator function of the novel RAD51- and RAD51B-binding protein, human EVL. *J. Biol. Chem.*, **284**, 14326–14336.
53. Takaku, M., Tsujita, T., Horikoshi, N., Takizawa, Y., Qing, Y., Hirota, K., Ikura, M., Ikura, T., Takeda, S. and Kurumizaka, H. (2011) Purification of the human SMN–GEMIN2 complex and assessment of its stimulation of RAD51-mediated DNA recombination reactions. *Biochemistry*, **50**, 6797–6805.
54. Hsieh, P., Camerini-Otero, C.S. and Camerini-Otero, R.D. (1992) The synapsis event in the homologous pairing of DNAs: RecA recognizes and pairs less than one helical repeat of DNA. *Proc. Natl Acad. Sci. USA*, **89**, 6492–6496.
55. Chow, S.A. and Radding, C.M. (1985) Ionic inhibition of formation of RecA nucleoprotein networks blocks homologous pairing. *Proc. Natl Acad. Sci. USA*, **82**, 5646–5650.
56. Tsang, S.S., Chow, S.A. and Radding, C.M. (1985) Networks of DNA and RecA protein are intermediates in homologous pairing. *Biochemistry*, **24**, 3226–3232.
57. Pezza, R.J., Camerini-Otero, R.D. and Bianco, P.R. (2010) Hop2-Mnd1 condenses DNA to stimulate the synapsis phase of DNA strand exchange. *Biophys. J.*, **99**, 3763–3772.
58. Kovalenko, O.V., Golub, E.I., Bray-Ward, P., Ward, D.C. and Radding, C.M. (1997) A novel nucleic acid-binding protein that interacts with human rad51 recombinase. *Nucleic Acids Res.*, **25**, 4946–4953.
59. Shinohara, M., Shita-Yamaguchi, E., Buerstedde, J.M., Shinagawa, H., Ogawa, H. and Shinohara, A. (1997) Characterization of the roles of the *Saccharomyces cerevisiae* RAD54 gene and a homologue of RAD54, RDH54/TID1, in mitosis and meiosis. *Genetics*, **147**, 1545–1556.
60. Tanaka, K., Hiramoto, T., Fukuda, T. and Miyagawa, K. (2000) A novel human rad54 homologue, Rad54B, associates with Rad51. *J. Biol. Chem.*, **275**, 26316–26321.